Supporting information

Electron-Induced State Conversion in Diamond NV Centers Measured with Pump-Probe Cathodoluminescence Spectroscopy

Magdalena Solà-Garcia[†], *Sophie Meuret*[†], *Toon Coenen*[†,§], *and Albert Polman*[†]

[†]Center for Nanophotonics, AMOLF, Science Park 104, 1098 XG, Amsterdam, The Netherlands
[§]Delmic BV, Kanaalweg 4, 2628 EB Delft, The Netherlands

1. Pump-probe measurements: set of spectra at 30 keV

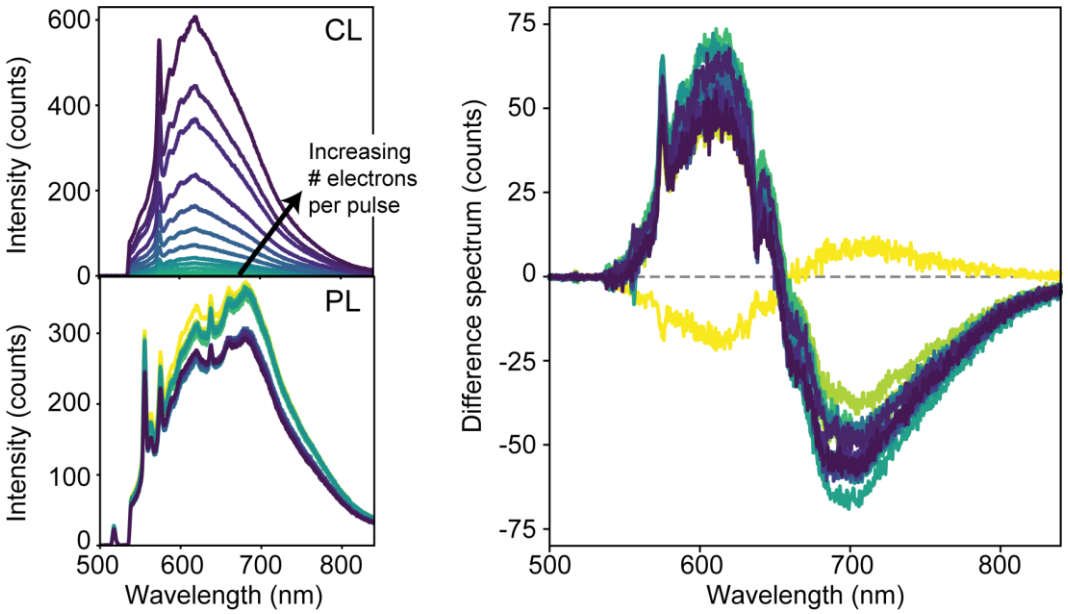

Figure S1. Pump-probe experiments performed with an electron energy of 30 keV. (a) Cathodoluminescence (CL), (b) Photoluminescence (PL) and (c) difference spectrum (PP – PL – CL, where PP stands for pump-probe). The colors of the curves indicate the number of electrons per pulse, going from 0 (yellow) up to 208 (dark purple). The difference spectrum reflects again the NV^- $\rightarrow NV^0$ conversion due to electron irradiation. Nevertheless, when performing these measurements at 30 keV we consistently observe deterioration of the sample after each CL measurement, as can be observed from the PL measurements (a) taken before each pump-probe measurement (and after each CL measurement). This deterioration of the sample can also be observed in the reference measurement (yellow curve, 0 electrons per pulse), which does not show a completely flat spectrum.

2. Laser power dependence of NV^- fraction

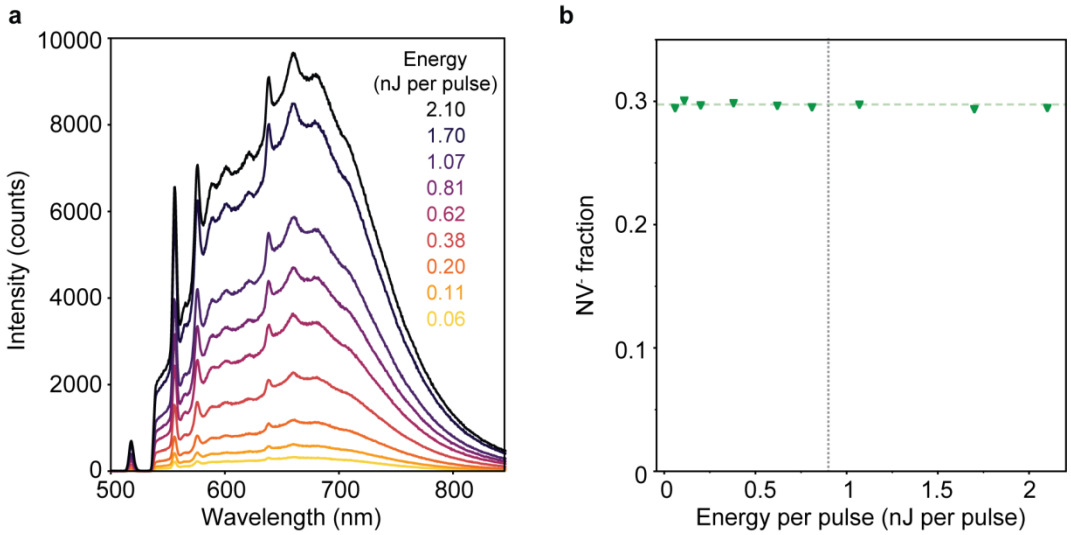

Figure S2. NV^- fraction as a function of the incident laser power. (a) PL spectra obtained at the same spot on the sample but different incident laser power, ranging from 0.06 up to 2.1 nJ per pulse. (b) NV^- fraction as a function of the energy per pulse, derived from the PL spectra in (a). The NV^- fraction remains constant for the different values of the incident power, indicating that optically-induced $NV^-\rightarrow NV^0$ conversion (or vice versa) is negligible in this case. The dotted gray line indicates the power at which the experiments from Fig. 2 were performed, while the dashed green line serves as a guide for the eye. These measurements were all acquired at the same spot on the sample, but different from the spot in which measurements from Figure 2 were performed, thus explaining why the NV^- fraction is different in both cases.

3. Pump-probe measurements vs. electron-laser delay

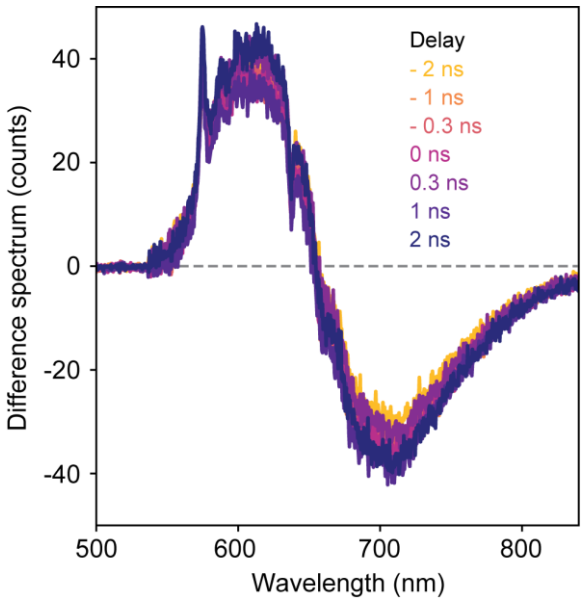

Figure S3. Difference spectrum obtained for different laser arrival times. The delay indicates the difference in arrival time of electrons and laser pulses to the sample, with negative delay indicating that the laser arrives before the electron beam. The $NV^-\rightarrow NV^0$ conversion is again observed in the difference spectrum, but there are no differences among the different delays, due to the fact that the electron-induced conversion has a timescale in the millisecond regime (Fig. 3b), much larger than the time between pulses in the experiments (198 ns at 5.04 MHz).

4. Transient of the back transfer dynamics

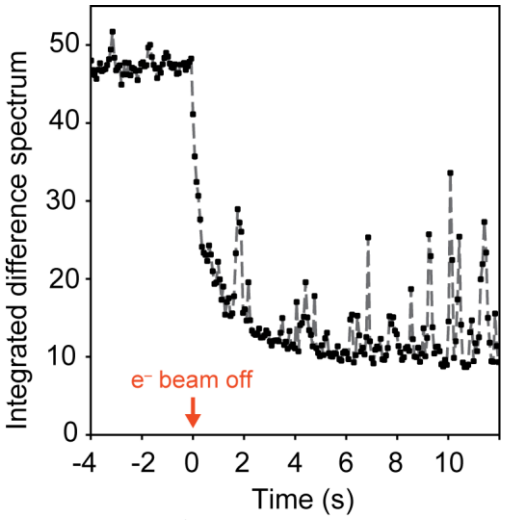

Figure S4. Temporal evolution of the $NV^0 \rightarrow NV^-$ back transfer after turning off the electron beam. The y-axis corresponds to the mean value of the intensity of each difference spectrum, after taking the absolute value. Each spectra is extracted every 70 ms during the measurement (Fig. 3b).

5. Data analysis

Absorption cross sections of NV^0 and NV^- at the excitation wavelength of λ=517 nm are estimated to be 2×10^{-17} cm^2 and 1.4×10^{-17} cm^2, respectively. In order to estimate these cross sections, first the NV^- and NV^0 contributions to the PL spectrum are disentangled by taking the normalized CL spectrum as the NV^0 spectral shape, and assuming that the remaining PL spectrum corresponds to the NV^- contribution. We then consider complementarity between emission and absorption spectra, and normalize by known absorption cross sections at the ZPL of each center.[1] The amount of excited NVs in PL from Figure 2b is calculated by considering the NV concentration (200 μm^{-3}), and a light collection depth of 23 μm. The NV^- population in the pump-probe measurements (Figure 2d) is obtained by fitting the PP spectra, after subtraction of the CL spectra, and considering the estimated absorption cross sections for the NV^- and NV^0 states. The fitting of the NV spectra are performed with a total of 14 Gaussian functions: for each NV state (NV^0 or NV^-), one Gaussian function is used to fit the ZPL and 6 broader Gaussian functions are used to account for the phonon replica. We estimate a relative error in the calculation of the NV^- population of <25%, due to uncertainties in the fitting procedure.

6. Model

Electron cascade simulations. The spatial distribution of the creation of bulk plasmons by the primary electron beam was obtained with the Monte Carlo-based simulation software Casino. We used a diamond density of 3.51 g cm^{-1} and bulk plasmon energy of 31 eV.[2] The beam diameter is set to 600 nm. From the simulations we derive an average of 70 bulk plasmons created per electron.

Model for diffusion of charge carriers. The evolution in space and time of the concentration of electron-hole pairs, $\rho_{eh}(r,t)$, is obtained by solving the three-dimensional diffusion equation in spherical coordinates, which gives:

$$\rho_{eh}(r,t) = \frac{a\sigma^3}{(2Dt+\sigma^2)^{3/2}} e^{-\frac{t}{\tau_R}} e^{-\frac{r^2}{4Dt+2\sigma^2}} \quad \text{(S1)}$$

where D is the carrier diffusion coefficient and τ_R the carrier lifetime, which accounts for the recombination of carriers. We consider $D = 1\ \mu m^2\ ns^{-1}$, as obtained from literature.[3,4] The parameters a and σ correspond to the amplitude and standard deviation of the 3D initial Gaussian distribution of carriers, derived from Casino simulations. In our case, $\sigma = 0.185$ µm and $a = 1404\ n_{el}$, where n_{el} is the number of electrons per pulse. We do not consider the effect of the diamond surface on the diffusion equation and recombination of carriers.

Discrete rate equation model. The concentration of NV^- as a function of position, r, and number of pulse, n, described by Equation 2 is derived by solving the rate equation:

$$\rho_-(r,n+1) = \rho_-(r,n) - \alpha(r)\rho_-(r,n) + \beta[\rho_-(r,0) - \rho_-(r,n)] \quad \text{(S2)}$$

Here, $\alpha(r)$ is described with Equation 3 and is obtained by considering the change in $\rho_-(r,t)$ between subsequent pulses only due to $NV^- \rightarrow NV^0$ conversion, i.e. $\alpha(r) = \rho_{-,conv}(r,T) - \rho_{-,conv}(r,0)$. This process is described with the rate equation:

$$\frac{\partial \rho_{-,conv}(r,t)}{\partial t} = -v_{th}\,\sigma_c\,\rho_{eh}(r,t)\,\rho_{-,conv}(r,t) \quad \text{(S3)}$$

Similarly, we derive the expression of $\beta = \rho_{-,back}(r,T) - \rho_{-,back}(r,0)$ from Equation 4 by considering the change in $\rho_-(r,t)$ during the time between two pulses only due to the $NV^0 \rightarrow NV^-$ back transfer, which is obtained by solving the rate equation:

$$\frac{\partial \rho_{-,back}(r,t)}{\partial t} = -\frac{1}{\tau_{back}}[\,\rho_{-,back}(r,t) - \rho_{-i}] \quad \text{(S4)}$$

In this description we assume that the change in $\rho_-(r,t)$ due to the $NV^- \rightarrow NV^0$ conversion and due to the $NV^0 \rightarrow NV^-$ back transfer are independent between subsequent pulses. This assumption is valid since the back transfer time (500 ms) is much longer than the time between pulses (198 ns). In order to compare the model with the experimental data, we calculate the steady state value, $\rho_-(r,\infty)$, and integrate over a cylindrical volume, with cross section corresponding to the Gaussian profile of the excitation beam (σ_{laser}=5 µm). Given that diamond is transparent at the excitation wavelength (λ=517 nm), absorption is only due to excitation of NV centers, thus NVs will be excited through the entire sample. Nevertheless, PL will only be effectively collected up to a certain depth, which becomes the fit parameter.

References

(1) Fraczek, E.; Savitzki, V. G.; Dale, M.; Breeze, B. G.; Diggle, P.; Markham, M.; Bennett, A.; Dhillon, H.; Newton, M. E.; Kemp, A. J. Laser Spectroscopy of NV- and NV0 Colour Centres in Synthetic Diamond. *Opt. Mater. Express* **2017**, *7*, 2571–2585.
(2) Klein, C. A. Radiation Ionization Energies in Semiconductors: Speculations about the Role of Plasmons. *Proc. Int. Conf. Phys. Semicond.* **1966**, *21*, 307–311.
(3) Malinauskas, T.; Jarasiunas, K.; Ivakin, E.; Ralchenko, V.; Gontar, A.; Ivakhnenko, S. Optical Evaluation of Carrier Lifetime and Diffusion Length in Synthetic Diamonds. *Diam. Relat. Mater.* **2008**, *17*, 1212–1215.
(4) Kozák, M.; Trojánek, F.; Malý, P. Optical Study of Carrier Diffusion and Recombination in CVD Diamond. *Phys. Status Solidi Appl. Mater. Sci.* **2013**, *210* (10), 2008–2015.